The Astrophysical Journal, 824:8 (8pp), 2016 June 10 doi:10.3847/0004-637X/824/1/8

EFFECT OF A RADIATION COOLING AND HEATING FUNCTION ON STANDING LONGITUDINAL OSCILLATIONS IN CORONAL LOOPS

S. Kumar[1], V. M. Nakariakov[1,2,3], and Y.-J. Moon[1]
[1] School of Space Research, Kyung Hee University, Yongin, 446-701, Gyeonggi, Korea; sanjaykumar@khu.ac.kr
[2] Centre for Fusion, Space and Astrophysics, Department of Physics, University of Warwick, Coventry CV4 7AL, UK
[3] Central Astronomical Observatory of the Russian Academy of Sciences at Pulkovo, 196140 St. Petersburg, Russia
Received 2015 May 7; accepted 2016 March 18; published 2016 June 3

ABSTRACT

Standing long-period (with periods longer than several minutes) oscillations in large, hot (with a temperature higher than 3 MK) coronal loops have been observed as the quasi-periodic modulation of the EUV and microwave intensity emission and the Doppler shift of coronal emission lines, and they have been interpreted as standing slow magnetoacoustic (longitudinal) oscillations. Quasi-periodic pulsations of shorter periods, detected in thermal and non-thermal emissions in solar flares could be produced by a similar mechanism. We present theoretical modeling of the standing slow magnetoacoustic mode, showing that this mode of oscillation is highly sensitive to peculiarities of the radiative cooling and heating function. We generalized the theoretical model of standing slow magnetoacoustic oscillations in a hot plasma, including the effects of the radiative losses and accounting for plasma heating. The heating mechanism is not specified and taken empirically to compensate the cooling by radiation and thermal conduction. It is shown that the evolution of the oscillations is described by a generalized Burgers equation. The numerical solution of an initial value problem for the evolutionary equation demonstrates that different dependences of the radiative cooling and plasma heating on the temperature lead to different regimes of the oscillations, including growing, quasi-stationary, and rapidly decaying. Our findings provide a theoretical foundation for probing the coronal heating function and may explain the observations of decayless long-period, quasi-periodic pulsations in flares. The hydrodynamic approach employed in this study should be considered with caution in the modeling of non-thermal emission associated with flares, because it misses potentially important non-hydrodynamic effects.

Key words: magnetohydrodynamics (MHD) – Sun: corona – Sun: oscillations – waves

1. INTRODUCTION

The main interest in magnetohydrodynamic (MHD) waves and oscillations in the solar atmosphere is connected with the possible role that waves play in the heating of the atmospheric plasma and with the exploitation of the plasma diagnostic potential of the waves (see De Moortel & Nakariakov 2012; Liu & Ofman 2014, for recent comprehensive reviews). An important class of coronal MHD oscillations is standing waves in coronal loops, where structuring of the plasma across the magnetic field acts as a waveguide, and the loop footpoints are effective mirrors that form a standing wave pattern.

Standing longitudinal oscillations in coronal loops were discovered as a periodic Doppler shift of hot coronal emission lines with the *SOHO*/SUMER spectrometer (Wang et al. 2002) and analyzed in detail by Wang et al. (2003a, 2003b). The oscillations, usually called "SUMER" oscillations (see Wang 2011 for a review), have periods in the range of about 5–40 minutes and are detected in long loops with lengths of 200–300 Mm. SUMER oscillations are seen to be very rapidly decaying, with the decay time being about the period of oscillations. The decay time was found to be linearly proportional to the period. The relative amplitudes of plasma flows in SUMER oscillations reach 100–300 km s^{-1}, which in some cases reaches 50% of the sound speed corresponding to the temperature of the emitting plasma. Simultaneous observations of Doppler shift and intensity variations showed a quarter-period phase shift in some cases (Wang et al. 2005). About half of the detected SUMER oscillations were found to be associated with flares (e.g., Wang 2011).

Oscillations similar to the SUMER oscillations have been detected in the Doppler shift of hot coronal emission lines observed with Yohkoh/BCS (Mariska 2005, 2006). Intensity oscillations with periods from 13 to 60 minutes in X-ray bright points were observed with Hinode/XRT by Kumar et al. (2011). Also, oscillations of soft X-ray intensity with periods of 12–30 minutes were found in the CORONAS-F/SPIRIT data (Akimov et al. 2005). Kim et al. (2012) observed a SUMER oscillation with a period of 12.6 minutes and a decay time of 16 minutes simultaneously in the microwave and EUV emission, with the Nobeyama Radioheliograph and SDO/AIA, respectively. Similar oscillations, with periods of about 32 minutes, were found in a white light curve of a stellar megaflare (Anfinogentov et al. 2013). The first direct detection of SUMER oscillations in imaging data was recently reported by Kumar et al. (2013). Similar oscillatory patterns have recently been detected in the soft-X-ray irradiance measurements data made with GOES (Dolla et al. 2012; Simões et al. 2015).

Ofman & Wang (2002) were first to interpret SUMER oscillations in terms of standing slow magnetoacoustic oscillations of coronal loops. The oscillation period was found to be determined by the length of the loop and the sound speed. If finite-β effects are accounted for, the sound speed should be replaced by the tube speed. The dependence of the period of SUMER oscillations on the magnetic field in the finite-β regime has been used for the seismological determination of the plasma parameter β in the oscillating loop (Wang et al. 2007). Damping of the oscillations was associated with thermal conduction.

The simple numerical 1D model of Ofman & Wang (2002) was further developed by Nakariakov et al. (2004), Tsiklauri et al. (2004), Mendoza-Briceño et al. (2004), Taroyan et al. (2005), Selwa et al. (2007), and Ogrodowczyk et al. (2009) who subsequently included radiative effects, gravitational stratification, effects of the chromosphere near the footpoints, and effects of the magnetic field curvature. It was shown that standing slow magnetoacoustic oscillations are easily excited by a localized deposition of heat or increase in the plasma pressure. Also, the simulations showed that the oscillations may occur in two different regimes, the well-known rapidly decaying oscillations, and decayless oscillations. In the latter regime, the oscillation is limited by the duration of the flare only. This regime has possibly been observed as the undamped oscillations of the flaring X-ray emission with a 20 minute period detected by Svestka (1994), a 143 s period detected by Terekhov et al. (2002), 25–48 s pulsations detected in the hard X-rays in the initial phase of three flares by Fárník et al. (2003b), 60 s variations of the Hα emission detected by Huang & Ji (2005), long-period ($\geqslant$60 s) variations of the radio and X-ray fluxes detected by Mészárosová et al. (2006), the 5 and 13.5 minute oscillatory modulation of the 8 mm emission revealed by Kislyakov et al. (2006), the persistent, semi-regular compressions of the flaring core region, modulating the plasma temperature and emission measure with a period of about 60 s, detected in soft X-rays and EUV by Simões et al. (2013), and the 4 minute pulsations of the hard X-ray, radio, and EUV emissions in a flare, detected by Li et al. (2015a).

For the theoretical analysis of waves, a useful alternative to full-scale numerical simulations is the method of an evolutionary equation. In this method, the wave evolution, e.g., its damping or amplification, wave shape deformation, and acceleration, is determined in terms of the intrinsic evolutionary mechanisms, such as dissipation, dispersion, nonlinearity, and activity of the medium. These evolutionary mechanisms are modeled by specific terms in the evolutionary equation. Specific expressions for the coefficients in front of these terms can be determined from a certain set of governing equations (e.g., MHD) or can be taken in a guessed, effective form, e.g., when some necessary but not understood physical processes (such as coronal heating) should be included in the model. Moreover, these coefficients could be determined empirically, from observations and then used to constrain the guessed expressions. In the coronal context, this approach has turned out to be successful in modeling wave phenomena in the corona, e.g., propagating longitudinal waves in coronal active region fans (Nakariakov et al. 2004; Tsiklauri et al. 2004; Afanasyev & Nakariakov 2015) and polar plumes (Ofman et al. 2000), nonlinear Alfvén waves in coronal holes (Nakariakov et al. 2000b).

For standing longitudinal waves in coronal loops, the evolutionary equation method was recently used by Ruderman (2013, referred to as R13 in the following discussion). The model designed in R13 is based on the asymptotic expansion with the use of the small parameter, determined by the weakness of the effects of nonlinearity and dissipation by finite thermal conduction and/or viscosity. It was shown that in this approximation the SUMER oscillation can be considered as a superposition of two oppositely propagating nonlinear waves governed by the Burgers equation. An interesting consequence of this study was a periodic movement of the position of the highest amplitude along the loop caused by the nonlinearity.

An important effect that needs to be accounted for in the description of standing longitudinal oscillations in coronal loops is the radiation from the perturbed plasma. The radiation is mainly controlled by the composition of the plasma and the presence of heavy, not fully ionized ions. In the context of longitudinal oscillations, the effect of radiative losses was analytically described by Bembitov et al. (2013), and shown to lead to enhanced damping. Dependence of the radiative losses on the plasma temperature and pressure is quite non-monotonic and includes segments with both positive and negative gradients (see, e.g., Figure 1 of Schure et al. 2009) and is additionally modified in the presence of heating. It has been known for a long time (e.g., Field 1965) that under certain circumstances (e.g., in the presence of heating), thermal instability can occur in a diffuse medium due to an imbalance between temperature-independent energy gains (i.e., heating) and temperature-dependent radiative losses. From the point of view of magnetoacoustic wave dynamics, peculiarities of the energy loss/gain function dependence on thermodynamical parameters (e.g., density and pressure) may lead to the amplification of oscillations and hence an increase in the nonlinearity (e.g., Nakariakov et al. 2000a). The balance of the radiative/heating effects and dissipation may lead to the appearance of stationary propagating nonlinear waves (auto-waves) of a saw-tooth shape (Chin et al. 2010; Molevich et al. 2011), slow magnetoacoustic auto-solitons (Nakariakov & Roberts 1999), and nonlinear resonant amplification of Alfvén waves (Zavershinsky & Molevich 2014).

The aim of this paper is to generalize the work of Ruderman (2013) accounting for isentropic effects based on the presence of an energy loss/gain function in the energy equation. In Section 2, we discuss the model and governing equations. In Section 3, we derive and analyze linear dispersion relations. In Section 4, we derive the nonlinear evolutionary equation. In Section 5, we study different regimes of the oscillations. The results obtained are summarized in Section 6.

2. GOVERNING EQUATIONS

In this study, we ignore 2D effects, such as the loop curvature and transverse non-uniformity, and consider longitudinal oscillations to be field-aligned acoustic oscillations. Effects of stratification are neglected too, and the loop is taken to be situated between 0 and L along the magnetic field directed along the z axis. The governing set of equations is the continuity, Euler, and energy equations,

$$\frac{\partial \rho}{\partial t} + \frac{\partial (\rho u)}{\partial z} = 0, \tag{1}$$

$$\frac{\partial u}{\partial t} + u\frac{\partial u}{\partial z} = -\frac{1}{\rho}\frac{\partial p}{\partial z} + \frac{1}{\rho}\frac{\partial}{\partial z}\rho\nu\frac{\partial u}{\partial z}, \tag{2}$$

$$\frac{\mathrm{d}p}{\mathrm{d}t} - \frac{\gamma p}{\rho}\frac{\mathrm{d}\rho}{\mathrm{d}t} = (\gamma - 1)[Q(\rho, p) + \nabla(\kappa\nabla T)], \tag{3}$$

$$p = \frac{k_\mathrm{B}}{m}T\rho, \tag{4}$$

where ρ is the plasma density, T is the temperature, p is the plasma pressure, u is the speed of a field-aligned bulk flow, γ is the adiabatic index, t is the time. The coefficients

$$\nu = \frac{4\eta_0}{3\rho}, \text{ and } \kappa = \frac{(\gamma - 1)m\kappa_\parallel}{\rho k_\mathrm{B}} \tag{5}$$

describe the viscosity and field-aligned thermal conduction, respectively, determined by the coefficients of the bulk viscosity η_0 and thermal conductivity $\kappa_\parallel$; and $Q(\rho, p)$ is the cooling/heating (the energy loss/gain) function that accounts for radiative cooling and unspecified coronal heating. In this study, the coefficients of the bulk viscosity η_0 and thermal conductivity $\kappa_\parallel$ are not specified because they are likely to be enhanced by microturbulent processes typical for plasmas. Equation (3) extends the governing equations used in R13 by including the cooling/heating function $Q(\rho, p)$.

In this study, we consider weak perturbations of the equilibrium, determined by the constant equilibrium density ρ_0, pressure p_0, and temperature T_0 that are assumed to be uniform along the loop. Hence, in the equilibrium, thermal conduction is zero. Thus, in the equilibrium, the cooling/heating function $Q(\rho_0, p_0) = 0$ (i.e., the heating compensates the radiative losses). The same equilibrium was considered, e.g., in Nakariakov et al. (2000a), Chin et al. (2010), and Molevich et al. (2011). The perturbations of the equilibrium have a form of field-aligned flows that satisfies the boundary conditions

$$u = 0 \text{ at } z = 0, L, \tag{6}$$

i.e., the chromosphere is considered to be a rigid wall for the longitudinal oscillations.

The perturbation amplitude is characterized by a dimensionless small parameter $\epsilon \ll 1$. The dissipative effects caused by finite thermal conduction and viscosity, and non-adiabatic effects caused by the radiative losses and heating, are considered to be of the order of ϵ too. Thus, the evolutionary equation will include quadratically nonlinear terms together with linear terms that represent the non-adiabatic processes. It is convenient to introduce the scaled coefficients at the dissipative terms as follows

$$\overline{\nu} = \epsilon^{-1}\nu \quad \text{and} \quad \overline{\kappa} = \epsilon^{-1}\kappa. \tag{7}$$

3. DISPERSION RELATIONS

Linearising the set of Equations (1)–(4)), we obtain

$$\frac{\partial \rho}{\partial t} + \rho_0 \frac{\partial u}{\partial z} = 0, \tag{8}$$

$$\frac{\partial u}{\partial t} + \frac{1}{\rho_0}\frac{\partial p}{\partial z} = \overline{\nu}\frac{\partial^2 u}{\partial z^2}, \tag{9}$$

$$\frac{\partial p}{\partial t} - \frac{\gamma p_0}{\rho_0}\frac{\partial \rho}{\partial t} = (\gamma - 1)\left[\tilde{a}_p p + \tilde{a}_\rho \rho + \overline{\kappa}\frac{\partial^2 T}{\partial z^2}\right], \tag{10}$$

$$p - \frac{k_B \rho_0}{m} T - \frac{k_B T_0}{m}\rho = 0, \tag{11}$$

where we used the linear terms in the Taylor expansion of the cooling/heating function Q near the equilibrium, with $\tilde{a}_\rho = \partial Q/\partial \rho$ taken at p_0 and $\tilde{a}_p = \partial Q/\partial p$ taken at ρ_0. Here, the variables p, ρ, u, and T are perturbations of the equilibrium state. In the following consideration, we assume that the terms on the right-hand side are assumed to be smaller than the terms on the left-hand side.

Assuming the harmonic dependence of the perturbed quantities $\sim\exp(-i\omega t + ikz)$, we obtain the dispersion relation

$$\omega^2 - C_s^2 k^2 - \frac{i(\gamma - 1)}{\rho_0}\left(\frac{\rho_0 \tilde{a}_\rho k^2}{\omega} + \tilde{a}_p \rho_0 \omega - \frac{\overline{\kappa} m \omega k^2}{k_B} + \frac{\overline{\kappa} T_0 k^4}{\omega}\right) + i\overline{\nu}\omega k^2 = 0, \tag{12}$$

where ω is the cyclic frequency, k is the wave number, and $C_s = (\gamma p_0/\rho_0)^{1/2}$ is the sound speed.

Considering that the left-hand side terms in Equations (9) and (10) are small, and hence the last two terms in Equation (12) are smaller than the first two terms, we obtain that $\omega \approx C_s k$, and determine the real and imaginary parts of the frequency as

$$\omega_R \approx C_s k, \tag{13}$$

$$\omega_I \approx \frac{(\gamma - 1)}{2} A - \left[\frac{(\gamma - 1)^2 m \overline{\kappa}}{2\gamma \rho_0 k_B} + \frac{\overline{\nu}}{2}\right] k^2, \tag{14}$$

respectively, where

$$A = \tilde{a}_\rho / C_s^2 + \tilde{a}_p \tag{15}$$

is the parameter determined by the heating/cooling function Q.

Equation (13) shows that the oscillation period is determined by the length of the loop, e.g., $P = 2\pi/\omega_R = \pi/C_s L$ for the fundamental longitudinal mode, and the sound speed. Equation (14) contains two terms. The second term on the right-hand side, which contains the thermal conductivity $\overline{\kappa}$ and viscosity $\overline{\nu}$ is always negative, and hence causes damping of the oscillation. The damping time is inversely proportional to k^2; thus, oscillations in shorter loops decay more rapidly. The first term on the right-hand side of (14) can be either positive or negative, depending at the local gradients of the cooling/heating function, A.

In the case when $A < 0$, this term contributes to damping. However, as it is independent of k, the damping caused by this term is the same in short and long loops. In the when $A > 0$, this term suppresses damping. When the condition

$$A = A_{crit} = \frac{2}{(\gamma - 1)}\left[\frac{(\gamma - 1)^2 \overline{\kappa} m}{2\gamma \rho_0 k_B} + \frac{\overline{\nu}}{2}\right] k^2 \tag{16}$$

is fulfilled, the oscillation becomes undamped. For $A > A_{crit}$, the plasma becomes unstable and the oscillation amplitude grows in time—the thermal over-stability occurs. The critical value A_{crit} corresponds to the threshold of the over-stability, which is determined by thermodynamical parameters of the plasma, the heating/cooling function and the length of the loop.

4. EVOLUTIONARY EQUATION FOR STANDING LONGITUDINAL OSCILLATIONS

Observations show that the relative amplitude of standing longitudinal oscillations in coronal loops reaches 30–50% (e.g., Wang 2011). Thus, it is necessary to account for nonlinear effects in the evolution of the oscillations. The presence of the small parameter allows us to perform the asymptotic analysis of weakly nonlinear, weakly isentropic standing longitudinal oscillations, following the methodology developed in R13.

Consider the nonlinear and non-adiabatic processes (the latter are caused by the finite viscosity and thermal conductivity, and the heating/cooling function) to operate at the slow time $t_1 = \epsilon t$. Thus, we look for a solution to Equations (1)–(4) in the form of expansions

$$f = f_0 + \epsilon\ f_1 + \epsilon^2 f_2 + ... \tag{17}$$

where f represents the quantities u, ρ, p, and T. The term f_0 represents the unperturbed state i.e., $f_0 = \text{const}$ with $u_0 = 0$.

4.1. First-order Approximation

Substituting expansion (17) in Equations (1)–(4), we collect terms of the same power of the small parameter ϵ. The first order approximation, after the elimination of all variables in favor of u_1 gives us the acoustic wave equation,

$$\frac{\partial^2 u_1}{\partial t^2} - C_s^2 \frac{\partial^2 u_1}{\partial z^2} = 0 \tag{18}$$

Equation (18) has the solution $u_1 = C_s\,[f(\xi) + g(\eta)]$, where

$$\xi = \omega(t - z/C_s),\ \eta = \omega(t + z/C_s) \tag{19}$$

are dimensionless variables, and $f(\xi)$ and $g(\eta)$ are arbitrary smooth functions that describe the waves travelling in the positive and negative directions z, respectively.

Applying the boundary conditions given by Equation (6), we obtain the solution in a form of standing waves,

$$u_1 = C_s[f(\xi) - f(\eta)], \tag{20}$$

which is a superposition of two waves propagating in opposite directions. The function $f(y)$ is periodic with the period 2π, which requires $\omega = \pi C_s/L$. This cyclic frequency corresponds to the fundamental longitudinal mode of a loop of length L, filled in with a uniform plasma with the sound speed C_s. The perturbations of other physical quantities are

$$\rho_1 = \rho_0[f(\xi) + f(\eta)],\ p_1 = \rho_0 C_s^2[f(\xi) + f(\eta)],$$
$$T_1 = (\gamma - 1)T_0[f(\xi) + f(\eta)]. \tag{21}$$

Solutions (20)–(21) correspond to the real part of the solution to the dispersion relation (13).

4.2. Second-order Approximation

Collecting terms of the order of ϵ^2 and again eliminating all variables in favor of u_2, we obtain

$$\frac{\partial^2 u_2}{\partial t^2} - C_s^2 \frac{\partial^2 u_2}{\partial z^2} = \frac{\omega^3[\gamma\overline{\nu} + (\gamma - 1)\overline{\kappa}]}{\gamma C_s}(f_-''' - f_+''')$$
$$- 2\omega C_s\left(\frac{\partial f_-'}{\partial t_1} - \frac{\partial f_+'}{\partial t_1}\right)$$
$$+ \omega^2 C_s[(\gamma + 1)(f_-'^2 - f_+'^2 + f_- f_-'' - f_+ f_+'')$$
$$+ (3 - \gamma)(f_- f_+'' - f_+ f_-'')] + (\gamma - 1)\omega C_s A(f_-' - f_+'), \tag{22}$$

where $f_- = f(\xi, t_1)$, $f_+ = f(\eta, t_1)$, and the prime denotes the partial derivatives of the function $f(y, t_1)$ with respect to the spatial coordinate y. The independent variable t_1 is the "slow" time that describes the evolution of the oscillations in the presence of the effects of non-adiabaticity and nonlinearity (i.e., the right-hand side of Equation (22)). Equation (22) is similar to Equation (30) of R13 with an additional term on the right-hand side, which accounts for the cooling/heating function via the parameter A. Equation (22) should be supplemented by the boundary conditions

$$u_2 = 0 \text{ at } z = 0, L. \tag{23}$$

The asymptotic expansion given by Equation (17) is valid when the second order terms f_2 do not experience a secular growth. Such a growth is possible if the right-hand side terms of Equation (22) are in resonance with the eigenfunctions of the boundary problem constituted by the left-hand side of Equation (22) and boundary conditions (23). This possibility is excluded by demanding the right-hand side of Equation (22) to be orthogonal to the eigenfunctions of Equation (22) with (23). Following the procedure described in R13 (similar methods have also been used in the solar context in the description of weakly nonlinear fast waves in Nakariakov & Oraevsky 1995; Nakariakov et al. 1997), we obtain the condition of the orthogonality,

$$\frac{\partial f}{\partial \tau} - 2\lambda f\frac{\partial f}{\partial y} - \frac{\partial^2 f}{\partial y^2} - \alpha f = 0, \tag{24}$$

where $\tau = t/t_{dl}$, and

$$t_{dl} = \frac{2\gamma L^2}{\pi^2[\gamma\nu + (\gamma - 1)\kappa]},\ \lambda = \frac{\epsilon\gamma(\gamma + 1)C_s L}{2\pi[\gamma\nu + (\gamma - 1)\kappa]},$$
$$\alpha = \frac{\epsilon\gamma(\gamma - 1)AL^2}{\pi^2[\gamma\nu + (\gamma - 1)\kappa]}. \tag{25}$$

Equation (24) is a generalized Burgers equation, similar to Equation (38) of R13, with the fourth, linear term accounting for the finite cooling/heating function. Solutions to Equation (24) with boundary conditions (6) should be substituted in Equation (20), which describes a standing oscillation and its evolution.

5. EVOLUTION OF STANDING LONGITUDINAL WAVES

An initial value problem constituted by Equations (24), (6), and (20), and the initial condition $f(y, 0) = -\sin(y)$ was solved numerically with the use of the standard procedure *pdede* in Matlab 8.5.1.[4] Numerical solutions $f(y, t_1)$ with the use of expressions (19) were substituted in Equation (20) to obtain the oscillations of the field-aligned velocity u_1.

Figures 1 and 2 show different regimes of the oscillations, determined by different combinations of the parameters of Equation (24). The top-left panels of both the figures show the decaying linear oscillation that was considered in detail in R13. Other panels show the effect of the cooling/heating function $Q(\rho, p)$. In the middle-left panels, the oscillation grows because of the thermal over-stability. In the top-right, the oscillations are undamped. This regime occurs when the profile of the dependence of the cooling/heating function on the density and pressure has a value given by condition (16). In this case, the damping caused by thermal conduction and viscosity is compensated by the amplification caused by the thermal over-stability. In the middle-right panels, the oscillation damps stronger than in the case without the cooling/heating function (the top-left panel). In this case, the profile of $Q(\rho, p)$ does not satisfy condition (16), and hence contributes to the oscillation

[4] mathworks.com/products/matlab/

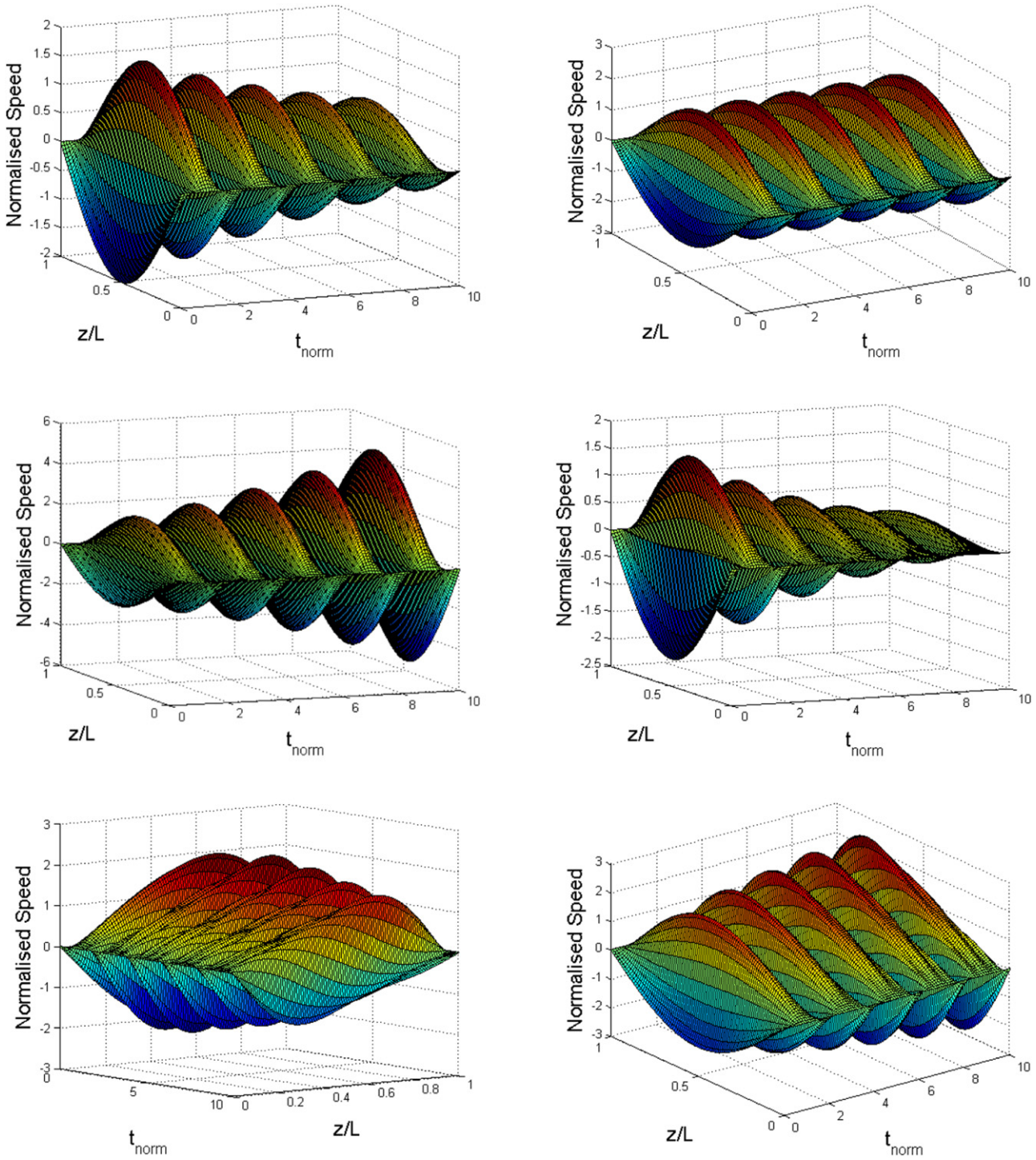

Figure 1. Different regimes of the evolution of the global longitudinal oscillation of a coronal loop, determined by different combinations of the parameters of nonlinearity and non-adiabaticity. The plasma speed is normalized at double the initial amplitude. The time is normalized at half the linear oscillation period. The spatial coordinate is normalized at the loop length L. Top row: the left panel shows a decaying linear oscillation ($\lambda = 0$, $\alpha = 0$); the right panel shows an almost undamped linear oscillation ($\lambda = 0$, $\alpha = 10$). Middle row: left panel shows a growing oscillation ($\lambda = 0$, $\alpha = 20$); the right panel shows an over-damped linear oscillation ($\lambda = 3$, $\alpha = -10$). Bottom row: the left panel shows an undamped highly nonlinear oscillation ($\lambda = 6$, $\alpha = 10$); the right panel shows a growing nonlinear oscillation ($\lambda = 3$, $\alpha = 15$).

damping. Despite the finite value of the nonlinear coefficient λ, the oscillation remains practically harmonic because it rapidly decreases in time. The bottom panels show nonlinear deformation of the oscillations caused by the finite amplitude. The plot in the bottom-left panel is rotated to make nonlinear deformation better visible. The nonlinearity manifests itself as the appearance of higher spatial harmonics of the oscillation, i.e. the instant snapshots of the oscillations can be considered as the sum of the fundamental mode $\sin(\pi z/L)$ and the nonlinearly generated modes $\sin(\pi N z/L)$ where the integer $N \geqslant 2$ is the spatial harmonic number. Figure 2 shows the gradual distortion of the oscillation profile that becomes anharmonic. For higher values of the nonlinear coefficient λ (see the bottom-left and bottom-right panels), the distortion is

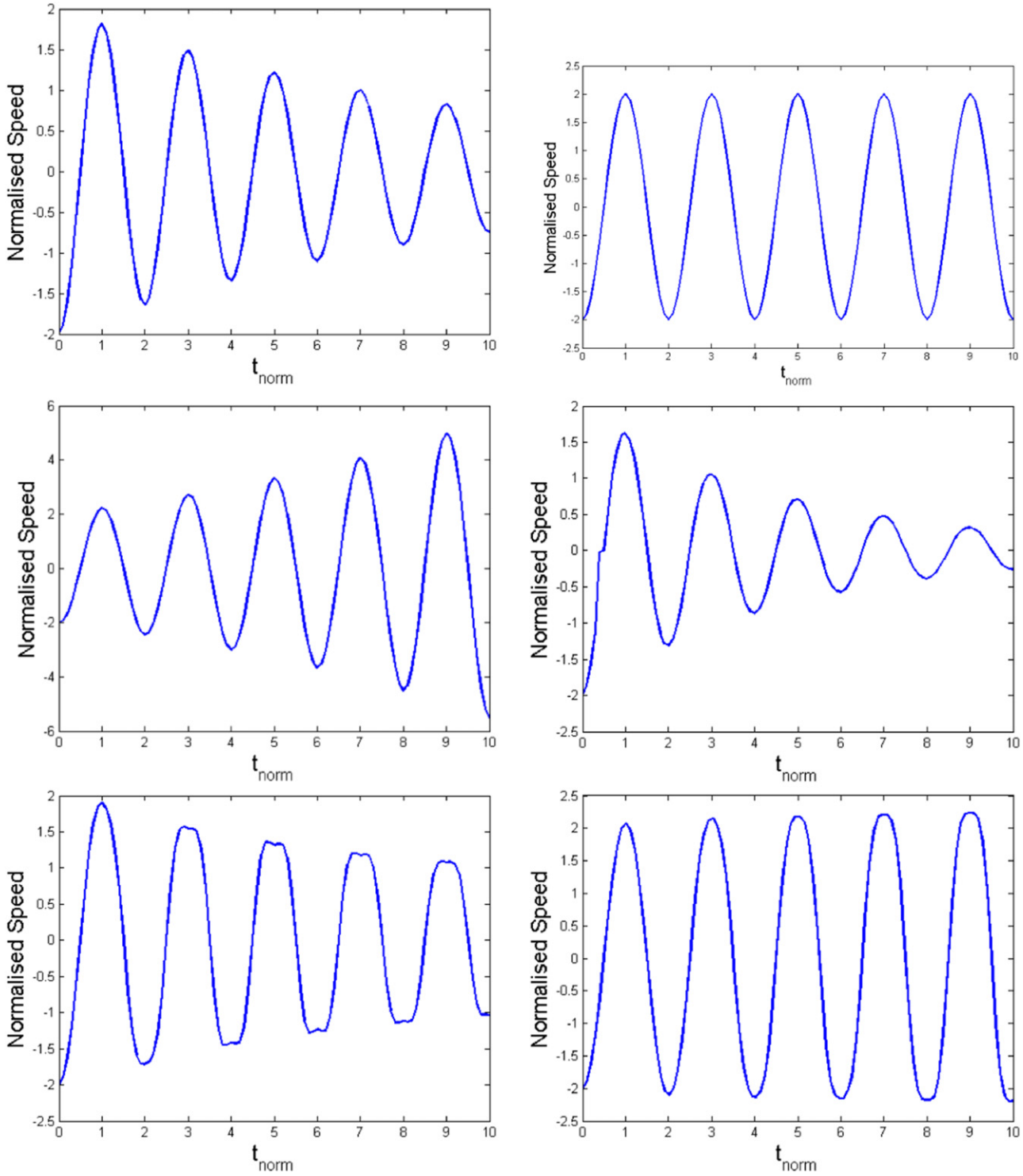

Figure 2. Variations of the longitudinal speed at the top of the loop in different regimes of the evolution of the global longitudinal oscillation, determined by different combinations of the parameters of nonlinearity and non-adiabaticity. The plasma speed is normalized at double the initial amplitude. The time is normalized at half the linear oscillation period. The panels correspond to the regimes shown in the corresponding panels of Figure 1.

more pronounced. Observationally, it would lead to the movement of the position of the highest amplitude along the loop from the top where it is in the fundamental mode.

6. DISCUSSION AND CONCLUSIONS

Our study shows that the cooling/heating function that accounts for radiation and unspecified heating of the coronal plasma can significantly affect longitudinal (slow magnetoacoustic) oscillations of coronal loops. The main contribution to this effect is caused by the gradient of this function at the equilibrium point on the thermodynamic parametric plane (e.g., the p–ρ plane). The specific dependence of the cooling/heating function on these parameters has not been established yet because it is connected with the enigmatic coronal heating

mechanism. Moreover, fine details of the radiative-loss function are also continuously updated following new and improved calculations of atomic data and transition rates (see, e.g., the discussion in Reale & Landi 2012). What is also important for our study is that the dependence of the radiative-loss function on the thermodynamical parameters is not steady, and even approximated dependences show steep positive and negative gradients for coronal conditions. Thus, we could treat the cooling/heating function as a free parameter in our study. Unfortunately, this uncertainty does not allow us to make any quantitative estimations, restricting our attention to the discussion of the possible regimes and their seismological implications only.

It should be pointed out that governing Equation (4) used in our derivation, as well as in R13, is rather simple, and may miss some important physical effects. In particular, these additional effects include the complex interactions between thermal and non-thermal plasmas in flares, and long-durational, in comparison with the oscillation period, field-aligned up- and downflows (e.g., Fárník et al. 2003a; Warren & Antiochos 2004; Li et al. 2015b). Thus, the specific values of the coefficients given by Equation (25) may need to be modified if these additional effects are taken into account. However, despite the possible changes in the governing equations, the general view of the evolutionary equation will be similar to Equation (24), which accounts for the intrinsic mechanisms responsible for the wave evolution: nonlinearity, dissipation, and activity. Our main finding is that the effects associated with the activity of the medium, modeled by the fourth term in Equation (24), may cause a dramatic change in the slow wave evolution and should not be neglected. Furthermore, in the context of this study, the specific value of the radiative losses is not important because the effect of the thermal over-stability is prescribed by the derivatives of the radiative losses and heating function with respect to the local thermodynamical parameters of the plasma.

It is clear that one of the obvious shortcomings of the presented analysis is the applicability of the effective fluid approach to flaring plasmas, which is not established and needs a dedicated study. On the other hand, the Burgers equation formalism is known to work well as the zero-order approximation even in a collisionless plasma (e.g., Hasegawa 1975). Also, the main intrinsic features of nonlinear wave dynamics, such as the nonlinear cascade and the appearance of dissipative structures, described by the generalized Burgers equation given by expression (24) are similar in very different environments.

In addition, the formalism developed in this study may be applied to the loops surrounding the flaring site, where the applicability of the fluid approach is justified. In this case, the oscillatory modulation of thermal emission (e.g., EUV, soft X-ray) comes from the variation of the plasma density and temperature. The oscillatory modulation of non-thermal emission (e.g., microwave, hard X-ray, γ-ray) could be produced by the modulation of the magnetic reconnection rate by a magnetoacoustic oscillation in a loop situated nearby the flaring site (Chen & Priest 2006; Nakariakov et al. 2006). In those scenarios, the modulation of non-thermal emission is produced by the periodic modulation of the plasma resistivity, caused by the modulation of the macroscopic plasma parameters, such as the density and temperature, by an MHD or acoustic wave. In addition, the periodic modulation of the density of the plasma, and hence the electron plasma frequency, by a slow magnetoacoustic wave, can periodically modulate the gyrosynchrotron emission produced by non-thermal electrons (Nakariakov & Melnikov 2006). Another possibility for the modulation of the non-thermal emission by a periodic variation of macroscopic plasma parameters in an MHD wave is the periodic variation of the magnetic mirror condition in the legs of flaring loops (Zaitsev & Stepanov 1982). Thus, admitting that the non-thermal emission is definitely caused by non-MHD effects, we would like to point out that its periodic modulation can be associated with the periodic variations of the macroscopic plasma parameters in MHD oscillations, considered in this paper.

We found that, depending on the specific gradient of the cooling/heating function at the thermal equilibrium, there are three main different regimes of longitudinal oscillations possible in coronal loops. The radiative cooling and heating effects can either increase the oscillation damping or suppress the damping caused by finite thermal conduction and viscosity. In the latter case, we can observe either undamped oscillations, or even an increase in the oscillation amplitude in time—the regime of thermal over-stability. In all these regimes, the oscillation period is determined by the loop length and temperature. We should point out that undamped oscillations have been detected in coronal oscillations during solar flares (e.g., Svestka 1994; Terekhov et al. 2002; Fárník et al. 2003b; Huang & Ji 2005; Kislyakov et al. 2006; Mészárosová et al. 2006; Simões et al. 2013; Li et al. 2015a), and hence could, at least in some cases, be attributed to this effect. In the undamped regime, the oscillation period remains determined by the length of the loop and the temperature of the plasma. For example, for a 120 s oscillation in a flaring plasma with a temperature of 20 MK, the length of the oscillating loop should be about 40 Mm for the fundamental harmonics and 80 Mm for the second spatial harmonics. It is necessary to mention that an undamped or growing regime of another MHD mode, the kink oscillation, has recently been discovered observationally (Wang et al. 2012; Nisticò et al. 2013) during non-flaring periods of time, while its nature remains unrevealed. Anyway, undamped kink oscillations are not likely to be responsible for the undamped or growing QPP detected in solar flares because that regime is observed during the quiet periods of the solar activity.

In contrast with the damping caused by finite thermal conduction and/or viscosity that decreases with the oscillation wavelength, the cooling/heating function is independent of the wavelength. It suggests that the undamped and over-stable regimes are more likely to occur in longer loops, in which the efficiency of the damping by thermal conduction and viscosity is lower. However, the realization of these regimes in specific situations depends on the specific thermodynamical parameters of the plasma in the oscillating loop. Also, the observational detection of an undamped or growing long-period oscillation is only possible in the case when the flaring emission in, e.g., the soft X-rays lasts longer than several cycles of the oscillation.

The nonlinear movement of the position of the highest amplitude along the loop, that was revealed in R13, becomes even more important in the case of undamped or growing oscillations. In those cases, nonlinear corrections get accumulated for a longer time, causing more significant departure from the harmonic shape of the oscillations.

Thermal over-stability can also lead to the excitation of oscillations. A gradual change of thermodynamical conditions in a loop could reach the instability's threshold (16), causing

the onset of the over-stability and hence an increase in the oscillation amplitude. In this reasoning, one could also take into account the possible onset of some plasma micro-instabilities caused, e.g., by plasma flows in the oscillations, resulting in an increase in the viscosity and thermal conductivity. This scenario could explain the sudden appearance of the oscillation and its rapid decay by the enhance dissipation. However, this discussion remains speculative until there has been a more detailed investigation of this possibility.

Our results demonstrate that the behavior of slow magnetoacoustic oscillations in coronal loops is sensitive to the peculiarities of the coronal cooling/heating function. Different dependences of the combination of the radiative cooling and heating on the plasma's thermodynamical parameters result in qualitatively different regimes of the oscillations (over-damped, undamped, and growing), providing us with a potential ground for the seismological diagnostics of the cooling/heating function in observations. This finding motivates a more detailed study of compressive oscillations in observational data. Special attention should be paid to the search for the undamped and growing regimes, similar to those described in similar to those described in, e.g., Svestka (1994); Terekhov et al. (2002); Fárník et al. (2003b); Huang & Ji (2005); Kislyakov et al. (2006); Mészárosová et al. (2006); Simões et al. (2013); Li et al. (2015a), the shape of the oscillation curve, and the appearance of higher spatial harmonics.

The significant limitations of the governing equations (discussed above) require further development of the model by including additional physical effects typical for flaring plasmas. The formalism for the derivation of evolutionary Equation (24) presented here provides one with a convenient starting point. Another limitation of the present study is the use of rigid-wall boundary conditions (6). However, if necessary, the developed formalism can be modified for the cases of open or asymmetric boundary conditions, which is out of scope of the present paper.

We would like to thank the anonymous referee for constructive comments. This work was supported by the BK21 plus program through the National Research Foundation (NRF) funded by the Ministry of Education of Korea, Basic Science Research Program through the NRF funded by the Ministry of Education (NRF-2013R1A1A2012763), NRF of Korea Grant funded by the Korean Government (NRF-2013M1A3A3A02042232), the Korea Meteorological Administration/National Meteorological Satellite Center (S.K., V.M. N., and Y.J.M.); and by the European Research Council under the SeismoSun Research Project No. 321141 (V.M.N.).

REFERENCES

Afanasyev, A. N., & Nakariakov, V. M. 2015, A&A, 573, A32
Akimov, L. A., Beletskii, S. A., Belkina, I. L., et al. 2005, ARep, 49, 579
Anfinogentov, S., Nakariakov, V. M., Mathioudakis, M., Van Doorsselaere, T., & Kowalski, A. F. 2013, ApJ, 773, 156
Bembitov, D. B., Veselovsky, I. S., & Mikhalyaev, B. B. 2013, Ge&Ae, 53, 1013
Chen, P. F., & Priest, E. R. 2006, SoPh, 238, 313
Chin, R., Verwichte, E., Rowlands, G., & Nakariakov, V. M. 2010, PhPl, 17, 032107
De Moortel, I., & Nakariakov, V. M. 2012, RSPTA, 370, 3193
Dolla, L., Marqué, C., Seaton, D. B., et al. 2012, ApJL, 749, L16
Fárník, F., Hudson, H. S., Karlický, M., & Kosugi, T. 2003a, A&A, 399, 1159
Fárník, F., Karlický, M., & Švestka, Z. 2003b, SoPh, 218, 183
Field, G. B. 1965, ApJ, 142, 531
Hasegawa, A. 1975, Physics and Chemistry in Space, Vol. 8, Plasma Instabilities and Nonlinear Effects (Berlin: Springer)
Huang, G., & Ji, H. 2005, SoPh, 229, 227
Kim, S., Nakariakov, V. M., & Shibasaki, K. 2012, ApJL, 756, L36
Kislyakov, A. G., Zaitsev, V. V., Stepanov, A. V., & Urpo, S. 2006, SoPh, 233, 89
Kumar, M., Srivastava, A. K., & Dwivedi, B. N. 2011, MNRAS, 415, 1419
Kumar, P., Innes, D. E., & Inhester, B. 2013, ApJL, 779, L7
Li, D., Ning, Z. J., & Zhang, Q. M. 2015a, ApJ, 807, 72
Li, Y., Ding, M. D., Qiu, J., & Cheng, J. X. 2015b, ApJ, 811, 7
Liu, W., & Ofman, L. 2014, SoPh, 289, 3233
Mariska, J. T. 2005, ApJL, 620, L67
Mariska, J. T. 2006, ApJ, 639, 484
Mendoza-Briceño, C. A., Erdélyi, R., & Sigalotti, L. D. G. 2004, ApJ, 605, 493
Mészárosová, H., Karlický, M., Rybák, J., Fárník, F., & Jiřička, K. 2006, A&A, 460, 865
Molevich, N. E., Zavershinsky, D. I., Galimov, R. N., & Makaryan, V. G. 2011, Ap&SS, 334, 35
Nakariakov, V. M., Foullon, C., Verwichte, E., & Young, N. P. 2006, A&A, 452, 343
Nakariakov, V. M., & Melnikov, V. F. 2006, A&A, 446, 1151
Nakariakov, V. M., Mendoza-Briceño, C. A., & Ibáñez, S. M. H. 2000a, ApJ, 528, 767
Nakariakov, V. M., Ofman, L., & Arber, T. D. 2000b, A&A, 353, 741
Nakariakov, V. M., & Oraevsky, V. N. 1995, SoPh, 160, 289
Nakariakov, V. M., & Roberts, B. 1999, PhLA, 254, 314
Nakariakov, V. M., Roberts, B., & Petrukhin, N. S. 1997, JPlPh, 58, 315
Nakariakov, V. M., Tsiklauri, D., Kelly, A., Arber, T. D., & Aschwanden, M. J. 2004, A&A, 414, L25
Nisticò, G., Nakariakov, V. M., & Verwichte, E. 2013, A&A, 552, A57
Ofman, L., Nakariakov, V. M., & Sehgal, N. 2000, ApJ, 533, 1071
Ofman, L., & Wang, T. 2002, ApJL, 580, L85
Ogrodowczyk, R., Murawski, K., & Solanki, S. K. 2009, A&A, 495, 313
Reale, F., & Landi, E. 2012, A&A, 543, A90
Ruderman, M. S. 2013, A&A, 553, A23
Schure, K. M., Kosenko, D., Kaastra, J. S., Keppens, R., & Vink, J. 2009, A&A, 508, 751
Selwa, M., Ofman, L., & Murawski, K. 2007, ApJL, 668, L83
Simões, P. J. A., Fletcher, L., Hudson, H. S., & Russell, A. J. B. 2013, ApJ, 777, 152
Simões, P. J. A., Hudson, H. S., & Fletcher, L. 2015, SoPh, arXiv:1412.3045
Svestka, Z. 1994, SoPh, 152, 505
Taroyan, Y., Erdélyi, R., Doyle, J. G., & Bradshaw, S. J. 2005, A&A, 438, 713
Terekhov, O. V., Shevchenko, A. V., Kuz'min, A. G., et al. 2002, AstL, 28, 397
Tsiklauri, D., Nakariakov, V. M., Arber, T. D., & Aschwanden, M. J. 2004, A&A, 422, 351
Wang, T. 2011, SSRv, 158, 397
Wang, T., Innes, D. E., & Qiu, J. 2007, ApJ, 656, 598
Wang, T., Ofman, L., Davila, J. M., & Su, Y. 2012, ApJL, 751, L27
Wang, T., Solanki, S. K., Curdt, W., Innes, D. E., & Dammasch, I. E. 2002, ApJL, 574, L101
Wang, T. J., Solanki, S. K., Curdt, W., Innes, D. E., & Dammasch, I. E. 2003a, AN, 324, 340
Wang, T. J., Solanki, S. K., Curdt, W., et al. 2003b, A&A, 406, 1105
Wang, T. J., Solanki, S. K., Innes, D. E., & Curdt, W. 2005, A&A, 435, 753
Warren, H. P., & Antiochos, S. K. 2004, ApJL, 611, L49
Zaitsev, V. V., & Stepanov, A. V. 1982, SvAL, 8, 132
Zavershinsky, D. I., & Molevich, N. E. 2014, TePhL, 40, 701